

Inflammation Impacts Androgen Receptor Signaling in Basal Prostate Stem Cells Through Interleukin 1 Receptor Antagonist

Timothy Ratliff (✉ tratliff@purdue.edu)

Purdue University <https://orcid.org/0000-0003-4221-5416>

Paula Cooper

Purdue University College of Veterinary Medicine <https://orcid.org/0000-0001-9201-1855>

Jiang Yang

Purdue University College of Veterinary Medicine

Hsing-Hui Wang

Purdue University College of Veterinary Medicine

Meaghan Broman

Purdue University West Lafayette

Gada Awdalkreem

Purdue University College of Veterinary Medicine

Gregory Cresswell

a. Department of Comparative Pathobiology, Purdue University, West Lafayette, Indiana b. Flow Cytometry Core Facility-GW Cancer Center, George Washington University, Washington DC

Liang Wang

Genentech Inc <https://orcid.org/0000-0002-4052-1316>

Emery Goossens

Purdue University

Nadia Atallah-Lanman

Purdue University <https://orcid.org/0000-0002-1819-7070>

Rebecca Doerge

Purdue University

Faye Zheng

Purdue University

Liang Cheng

Brown University <https://orcid.org/0000-0001-6049-5293>

Scott Crist

Purdue University West Lafayette

Robert Braun

Jackson Laboratory <https://orcid.org/0000-0003-3856-9465>

Travis Jerde

Indiana University School of Medicine

Article

Keywords: prostate, stem cells, inflammation, androgen receptor, interleukin 1 receptor antagonist

Posted Date: December 15th, 2023

DOI: <https://doi.org/10.21203/rs.3.rs-3539806/v1>

License:   This work is licensed under a Creative Commons Attribution 4.0 International License.

[Read Full License](#)

Additional Declarations: There is **NO** Competing Interest.

1 **Inflammation Impacts Androgen Receptor Signaling in Basal Prostate Stem Cells**
2 **Through Interleukin 1 Receptor Antagonist**

3
4 Paula O. Cooper^{1,2,7}, Jiang Yang^{1,2,7,*}, Hsing-Hui Wang^{1,2,7}, Meaghan M. Broman^{1,2}, Gada D.
5 Awdalkreem^{1,2}, Gregory M. Cresswell^{1,2}, Liang Wang³, Emery Goossens⁴, Nadia A. Lanman^{1,2},
6 Rebecca W. Doerge⁴, Faye Zheng⁴, Liang Cheng⁵, Scott A. Crist^{1,2}, Robert E. Braun⁶, Travis J.
7 Jerde^{3,*}, Timothy L. Ratliff^{1,2,*}

8
9 ¹Department of Comparative Pathobiology, College of Veterinary Medicine, Purdue University,
10 West Lafayette, IN 47907, USA

11 ²Purdue Institute for Cancer Research, West Lafayette, IN 47907, USA

12 ³Department of Pharmacology and Toxicology, Department of Urology, Department of
13 Microbiology and Immunology, Indiana University School of Medicine, Indianapolis, IN 46202,
14 USA

15 ⁴Department of Statistics, Purdue University, West Lafayette, IN 47907, USA

16 ⁵Department of Pathology and Laboratory Medicine, Indiana University School of Medicine,
17 Indianapolis, IN 46202, USA

18 ⁶The Jackson Laboratory, Bar Harbor, ME 04609, USA

19 ⁷These authors contributed equally to the manuscript.

20
21 *Co-Corresponding authors:

22 Timothy L. Ratliff, Ph.D.
23 Department of Comparative Pathobiology
24 Purdue University College of Veterinary Medicine
25 Purdue Institute for Cancer Research
26 Bindley Bioscience Center, Rm 190
27 1203 Mitch Daniels Blvd.
28 West Lafayette, IN 47907, USA
29 Phone: 765-494-9129
30 Email: tratliff@purdue.edu

1

2 Travis J. Jerde, Ph.D.
3 Department of Pharmacology and Toxicology
4 Department of Urology
5 Department of Microbiology and Immunology
6 Indiana University School of Medicine
7 635 Barnhill Drive
8 Indianapolis, IN 46202, USA
9 Phone: 317-274-1534
10 Email: tjjerde@iu.edu

11

12 Jiang Yang, Ph.D.
13 Department of Comparative Pathobiology
14 Purdue University College of Veterinary Medicine
15 Purdue Institute for Cancer Research
16 Bindley Bioscience Center, Rm 181
17 1203 Mitch Daniels Blvd.
18 West Lafayette, IN 47907, USA
19 Phone: 765-494-7284
20 Email: yang1491@purdue.edu

21

22 Current address:

23 POC: Department of Biochemistry and Molecular Medicine, School of Medicine and Health
24 Sciences, The George Washington University, Washington, DC 20037, USA

25 HHW: Immune Monitoring and Genomics Facility, Lineberger Comprehensive Cancer Center,
26 University of North Carolina School of Medicine, Chapel Hill, NC 27599, USA

27 GMC: Flow Cytometry Core Facility, School of Medicine and Health Sciences, The George
28 Washington University, Washington, DC 20037, USA

29 RWD: Provost, Rensselaer Polytechnic Institute, Troy, NY 12180, USA

30 FZ: Sorcerero, Inc., K St NW, 3rd Floor, Washington, DC 20005, USA

31 LC: Department of Pathology and Laboratory Medicine, Brown University Division of Biology
32 and Medicine, Providence, RI 02912, USA

33 SAC: Carver College of Medicine, Fraternal Order of Eagles Diabetes Research Center,
34 University of Iowa, Iowa City, IA 52242, USA

35

1 Key words: prostate, stem cells, inflammation, androgen receptor, interleukin 1 receptor

2 antagonist

3

1 **Abstract:**

2 The majority of patients with benign prostate hyperplasia (BPH) exhibit chronic prostate
3 inflammation and the extent of inflammation correlates with the severity of symptoms. How
4 inflammation contributes to prostate enlargement and/or BPH symptoms and the underlying
5 mechanisms are not clearly understood. We established a unique mouse model Prostate
6 Ovalbumin Expressing Transgenic 3 (POET3) that mimics chronic non-bacterial prostatitis in
7 men to study the role of inflammation in prostate hyperplasia. After the injection of ovalbumin
8 peptide-specific T cells, POET3 prostates exhibited an influx of inflammatory cells and an
9 increase in pro-inflammatory cytokines that led to epithelial and stromal hyperplasia. We have
10 previously demonstrated with the POET3 model that inflammation expands the basal prostate
11 stem cell (bPSC) population and promotes bPSC differentiation in organoid cultures. In this
12 study, we investigated the mechanisms underlying the impact of inflammation on bPSC. We
13 found that AR activity was enhanced in inflamed bPSC and was essential for bPSC
14 differentiation in organoid cultures. Most importantly, we identified, for the first time, interleukin 1
15 receptor antagonist (IL-1RA) as a key regulator of AR in basal stem cells. IL-1RA was one of the
16 top genes upregulated by inflammation and inhibition of IL-1RA abrogated the enhanced AR
17 nuclear accumulation and activity in organoids derived from inflamed bPSC. The mirroring
18 effects of IL-1RA recombinant protein and IL-1 α neutralizing antibody suggest that IL-1RA may
19 function by antagonizing IL-1 α inhibition of AR expression. Furthermore, we established a
20 lineage tracing model to follow bPSC during inflammation and under castrate conditions. We
21 found that inflammation induced bPSC proliferation and differentiation into luminal cells even
22 under castrate conditions, indicating that AR activation driven by inflammation in bPSC is
23 sufficient for their proliferation and differentiation under androgen-deprived conditions. However,
24 proliferation of the differentiated bPSC in the luminal layer significantly diminished with
25 castration, suggesting inflammation may not maintain AR activity in stromal cells, as stromal

1 cells deprived of androgen after castration could no longer provide paracrine growth factors
2 essential for luminal proliferation. Taken together, we have discovered novel mechanisms
3 through which inflammation modulates AR signaling in bPSC and induces bPSC luminal
4 differentiation that contributes to prostate hyperplasia.

1 Introduction

2 The coexistence of inflammation and benign prostate hyperplasia (BPH) are well
3 documented^{1,2}. The majority of BPH patients exhibit chronic inflammation and the extent of
4 inflammation correlates with the severity of symptoms^{3,4}. However, a direct link between
5 inflammation and BPH remains an open question. Inflammation may contribute to BPH through
6 multiple mechanisms². One important mechanism may be through its modulation of prostate
7 stem cell populations, which have long been implicated in hyperproliferative diseases^{5,6}.

8 Stem cells within the prostate basal epithelium (basal prostate stem cells, bPSC) can
9 differentiate into both luminal and basal lineages in *in vitro* organoid cultures and have been
10 shown to contribute to the repair and recovery of the luminal epithelium in various animal
11 models for prostate diseases and injuries. For example, lineage tracing models tracking bPSC
12 have shown that these stem cells contribute to the repair of prostate luminal epithelium in an
13 induced luminal anoikis model⁷, or to a smaller extent, during the castration-regeneration
14 cycles^{8,9}. We and others have shown that inflammation greatly impacts the behavior of bPSC.
15 In our previous studies, we established a unique mouse model (Prostate Ovalbumin Expressing
16 Transgenic 3 (POET3)) that closely models human chronic non-bacterial prostatitis, the most
17 commonly diagnosed clinical prostatitis¹⁰. After adoptive transfer of pre-activated ovalbumin
18 peptide-specific CD8+ T cells isolated from the spleens of OT-1 transgenic mice, this model
19 experiences an influx of inflammatory immune cells into the prostate, including CD8+, CD4+,
20 and Foxp3+/CD4+ T cells as well as myeloid-derived suppressor cells (MDSC), and an increase
21 in pro-inflammatory cytokine production¹⁰, which leads to the development of epithelial and
22 stromal hyperplasia. Along with the induction of inflammation, we observed a significant
23 expansion of bPSC population, which produced larger and more differentiated organoids
24 (resembling type II tubule-like organoids, based on classifications by Kwon *et al.*¹¹) in a 3D
25 androgen-free culture system¹². Inflammation-induced expansion of the bPSC population and
26 enhanced bPSC differentiation capability were also described in other inflammation models,

1 including bacteria-induced acute prostatitis^{13, 14}. The mechanisms underlying the impact of
2 inflammation on bPSC and how the bPSC contributes to prostate hyperplasia are still poorly
3 understood.

4 The androgen receptor (AR) plays a critical role in prostate homeostasis and
5 maintenance. Drugs that target androgen synthesis and signaling remain as important
6 treatments for both benign and malignant prostate diseases. In addition to its strong presence in
7 the epithelium, AR activation in prostate stromal cells releases paracrine growth factors (e.g.
8 NRG, FGF, IGF, EGF), which act on the corresponding receptors on luminal epithelial cells and
9 contribute to epithelial and stromal expansion and the regeneration of luminal epithelium during
10 the castration-regeneration cycle^{8, 9}. While strong AR nuclear presence is prevalent in luminal
11 epithelial cells, AR staining is observed in about half of total basal epithelial cells⁸. Not
12 surprisingly, AR is dispensable in the regression and recovery of basal epithelium during the
13 castration and regeneration process⁸. However, AR is required for the differentiation of bPSC
14 into luminal epithelial cells during the castration-regeneration cycle, as the number of lineage-
15 traced bPSC in the luminal layer during regeneration was significantly reduced in basal
16 epithelium-specific AR knockout mice⁸.

17 In the current study, we determined that both AR expression and activity were markedly
18 stimulated in bPSC isolated from inflamed prostates in our POET3/OT-1 prostatitis model. With
19 both organoid cultures and *in vivo* lineage tracing models, we have shown that AR signaling is
20 essential for the differentiation of bPSC into luminal epithelial cells during prostatitis and
21 inflammation stimulates AR even under androgen-deprived castrate conditions, which is
22 sufficient to trigger basal to luminal differentiation. Most importantly, we identified a novel
23 mechanism for AR modulation in bPSC where interleukin-1 receptor antagonist (IL-1RA)
24 expressed by bPSC was shown to enhance nuclear localization of AR, modulate AR-dependent
25 gene expression and function as the driver for bPSC luminal differentiation.

1 **Results**

2 **AR activity is elevated in prostate basal stem cells isolated from inflamed POET3 mice**

3 Given the critical function of AR in prostate homeostasis and stem cell differentiation, we
4 assessed the impact of inflammation in our POET3/OT-1 prostatitis model on AR signaling in
5 bPSC population. As shown in Fig. 1A, bPSC were identified via flow cytometry as CD45-
6 /CD31-, Sca-1+ and CD49f+ (middle panels). A significantly higher percentage of the inflamed
7 bPSC was positive for full-length AR identified with an antibody against C-terminal AR (Fig. 1A,
8 right panels, and 1B). Consistent with the flow cytometry data, immunoblot using an antibody
9 against N-terminal AR detected an AR band at about 120 kDa in inflamed bPSC, while,
10 consistent with previous characterization studies¹⁵, the naïve bPSC produced a strong band of
11 degraded AR at about 70 kDa (Fig. 1C). To verify increased AR activity, a qRT-PCR array for
12 AR signaling target genes was used to compare the naïve and inflamed bPSC samples. The
13 resulting heatmap illustrates the differential expression of various AR target genes between
14 naïve and inflamed bPSC (Supplemental Fig. 1A), with twenty-three genes, including *Tmprss2*,
15 significantly upregulated in inflamed bPSC (Fig. 1D, Supplemental Table 1). The upregulation of
16 *Tmprss2* in inflamed bPSC was further verified with qRT-PCR and its level in inflamed bPSC
17 was comparable with the level observed in luminal epithelial cells (Fig. 1E). We further
18 examined other canonical luminal AR target genes via qRT-PCR and found that the canonical
19 target *Nkx3-1* remained at similar levels between naïve and inflamed bPSC (Fig. 1E). Therefore,
20 these data demonstrate that both AR levels and activity were increased in inflamed bPSC and
21 AR activation driven by inflammation may trigger a different target gene program.

22

23 **Inflammation-driven AR activity is sustained in bPSC-derived organoids under androgen-** 24 **deficient condition and is essential for the organoid growth and differentiation**

25 To examine the persistence of altered AR signaling upon removal from the inflammatory
26 environment and circulating androgens, bPSC were isolated from naïve or inflamed prostates

1 and cultured under defined and serum-free organoid culture conditions in the absence of
2 androgen¹². AR expression and activity were analyzed in formed organoids. Immunoblot of
3 lysates from naïve or inflamed organoids revealed that full-length AR was elevated in inflamed
4 organoids and its levels were further increased with synthetic AR ligand R1881 (Fig. 1F). R1881
5 was able to stabilize AR in the naïve organoids, with band shifting from the degraded product at
6 70 kDa to full-length AR at 120 kDa¹⁵ (Fig. 1F). Consistent with the increase in total AR protein
7 level, a significantly higher percentage of cells with overall or nuclear AR staining was observed
8 in organoids derived from inflamed bPSC compared to those from naïve bPSC (Fig. 1G, with
9 quantitation in Fig. 4C, Naïve_control and Inflamed_control groups), indicating that AR remains
10 active in inflamed organoids even in the absence of androgen and inflammatory cells.
11 Compared to the PCR array data collected from freshly isolated bPSC (Fig. 1D), AR target gene
12 array with the organoids identified a smaller, yet intriguing set of significantly upregulated AR
13 responsive genes in the inflamed organoids (Fig. 1H, Supplemental Fig. 1B, Supplemental
14 Table 2). The modulation of these target genes confirmed the enhanced AR activity in organoids
15 derived from inflamed bPSC. Furthermore, the difference in AR-responsive genes between
16 freshly isolated bPSC and organoids suggests that AR may perform distinct functions in
17 organoid growth and differentiation in androgen-depleted conditions.

18 Given the strong expression of full-length AR in the inflamed bPSC and organoids,
19 coupled with induced AR target gene expression and increased bPSC differentiation, we
20 reasoned that the effects inflammation exerted on bPSC may be mediated through AR. To verify
21 the requirement for AR signaling in inflammation-driven organoid proliferation and
22 differentiation, naïve or inflamed bPSC were treated with the clinical AR antagonist,
23 Enzalutamide (Enz), for the duration of organoid culture. AR inhibition resulted in a significant
24 74% reduction in inflamed organoid formation and 94% reduction in naïve organoid formation
25 (Fig. 2A). These data suggest that the presence of low AR activity in naïve bPSC and organoids
26 is essential for organoid formation, which is consistent with a previous report on the

1 indispensable role of AR during basal to luminal differentiation using conditional AR knockout
2 mouse models⁸. Of note, inflamed bPSC were able to form a significantly larger number of
3 organoids compared to naïve bPSC in the presence of Enz, suggesting that inflamed bPSC are
4 more resistant to Enz treatment, likely due to their higher nuclear AR activity (Fig. 1G and 4C).
5 In addition to reduced organoid number, Enz-treated inflamed organoids showed a significant
6 reduction in size (Fig. 2B). Histopathological assessment further revealed an altered organoid
7 morphology, with Enz-treated inflamed organoids more closely resembling naïve organoids.
8 Organization and cellular stratification present in the inflamed organoids were reduced with Enz
9 treatment, as reflected by the decreased percentage of tubule-like organoids with hollow lumens
10 (Fig. 2C,D). Immunofluorescence staining verified the enhanced luminal differentiation in
11 inflamed organoids with distinct central Cytokeratin 8 (CK8) (luminal epithelial marker) positive
12 layers and peripheral CK5 (basal epithelial marker) positive layers (Fig. 2E). Enz treatment
13 resulted in more solid organoids composed of CK8 and CK5 double positive cells (Fig. 2C,D,E),
14 indicating that Enz blocked the complete differentiation into CK8+, CK5- luminal cells and
15 trapped the stem cells in a transitional state. In addition to treatments with pharmacological AR
16 inhibitors, bPSC were also isolated from *Ar_flox/y* mice and infected with lentivirus encoding Cre
17 recombinase. The consequent knockout of AR resulted in significantly reduced number of
18 organoids (Fig. 4F, control and AR_floxed groups). Furthermore, based on a protocol described
19 by Henry *et al.*¹⁶, we enriched PSC from human prostate samples with flow cytometry as CD45-,
20 EpCAM+, CD26- and CD49f+ cells. Treatment with Enz significantly decreased human organoid
21 formation by 84% (Fig. 2F). Taken together, these results from the inflamed bPSC-derived
22 organoids with manipulated AR established the underlying role of AR in inflammation-driven
23 basal stem cell proliferation and differentiation.

24

25

1 **IL-1RA is upregulated in bPSC from inflamed prostates and regulates AR activity and** 2 **differentiation in bPSC-derived organoids**

3 We next investigated the mechanisms that underlie the inflammation-driven changes in
4 the basal stem cells, including the enhanced AR activity and differentiation, by conducting a
5 single-cell RNA sequencing (scRNA-seq) analysis comparing freshly sorted naïve and inflamed
6 bPSC. Along with a multitude of intriguing gene expression changes (Supplemental Table 3), IL-
7 1 receptor antagonist (IL-1RA, gene name *Il1rn*) and IL-1 α (gene name *Il1a*) were identified
8 among the top differentially expressed genes between naïve and inflamed bPSC (Fig. 3A,
9 arrows, and Fig. 3B), whereas IL-1 β was not detectable in either naïve or inflamed bPSC. IL-1
10 receptor 1 (IL-1R1, gene name *Il1r1*) was also identified as significantly upregulated in inflamed
11 bPSC by scRNA-seq analysis (Fig. 3B). The upregulation of IL-1RA (both the soluble and
12 intracellular isoforms) and IL-1 α was also confirmed with qRT-PCR (Fig. 3C). Consistent with its
13 transcript expression, IL-1RA protein could be detected using ELISA in the lysates from
14 inflamed bPSC but was undetectable in naïve bPSC lysates (Fig. 3D). IL-1 α protein was not
15 detectable by ELISA in the lysates of either naïve or inflamed bPSC, possibly because most of
16 IL-1 α was released by the bPSC.

17 Given the impact of IL-1 on AR expression in prostate cancer cells and its impact on
18 prostate cancer cell proliferation¹⁷⁻²⁰, we reasoned that IL-1RA or IL-1 α may modulate AR
19 expression in inflamed bPSC and influence organoid growth and differentiation. We first initiated
20 studies to evaluate the impact of IL-1RA on the differentiation and AR activity in naïve
21 organoids. Treatment of naïve bPSC cultured for organoid development with IL-1RA
22 recombinant protein produced organoids with distinct cellular stratification, more closely
23 resembling those from inflamed bPSC (Fig. 4A). IL-1RA treatment also induced a significant
24 increase in the number of formed organoids (Fig. 4B). Naïve organoids treated with an IL-1 α
25 neutralizing antibody (Ab), which blocks the binding of IL-1 α to its receptor, IL-1R1, and mimics

1 the function of IL-1RA, showed more differentiated structure and increased number as well,
2 resembling the results from IL-1RA treatment (Fig. 4A,B). Consistent with the inhibitory function
3 of IL-1 α in organoid formation, treatment with IL-1 α significantly reduced the number of
4 organoids formed with both naïve and inflamed bPSC (Supplemental Fig. 2). These data
5 suggest that IL-1RA promotes bPSC organoid growth and differentiation by antagonizing the
6 inhibitory effects of IL-1 α .

7 We next assessed the impact of IL-1RA and IL-1 α on AR in bPSC-derived organoids.
8 AR levels and nuclear localization in organoids were analyzed with immunofluorescence. The
9 number of cells with positive AR staining, and more importantly, number of cells with AR nuclear
10 localization were significantly increased in naïve organoids treated with IL-1RA to the level
11 comparable with inflamed organoids (Fig. 4C). Addition of IL-1RA to inflamed organoids derived
12 from inflamed bPSC that expressed higher level of IL-1RA did not have any significant effects
13 on AR (Fig. 4C). The effects of IL-1RA on AR levels in naïve organoids were mirrored by those
14 induced by an IL-1 α neutralizing Ab (Fig. 4D), suggesting that IL-1RA exerts its action on AR by
15 blocking IL-1 α . Consistent with IL-1RA's effects on AR nuclear localization, *Steap4*, an AR
16 target gene identified in organoids (Fig. 1H), was found to be significantly induced in naïve
17 organoids with IL-1RA treatment and the upregulation was abolished in the presence of Enz
18 (Fig. 4E). In contrast, an antibody that neutralized IL-1RA activity was observed to inhibit both
19 total AR level and AR nuclear localization in inflamed organoids, demonstrating that IL-1RA is
20 the driver of AR activation during inflammation (Fig. 4D). Data supporting the indispensable role
21 of AR downstream of IL-1RA were also obtained with genetic deletion of AR in the organoids.
22 When bPSC were isolated from *Ar_flox/y* transgenic mice and AR was removed from the
23 organoids with Cre recombinase lentivirus infection, IL-1RA could no longer stimulate growth in
24 AR knockout organoids (Fig. 4F). These data demonstrate that IL-1RA, which is upregulated in

1 bPSC during inflammation, is responsible for activated AR in this stem cell population and
2 enhanced organoid growth and differentiation.

3

4 **Inflammation in a prostatitis mouse model promotes the basal to luminal differentiation**

5 We have previously reported in our POET3/OT-1 prostatitis model that prostate
6 inflammation expanded the size of the bPSC population *in vivo*¹². To investigate whether
7 inflammation increases the number of bPSC by stimulating their proliferation, POET3 mice were
8 injected with pre-activated OT-1 T cells and BrdU incorporation was analyzed 7 days later at the
9 peak of the inflammation. Percentage of proliferating BrdU+ cells in the bPSC population was
10 found to be significantly increased in inflamed prostates compared to naïve prostates (Fig. 5A).

11 In addition to having a larger population size, we have also shown previously that bPSC
12 isolated from inflamed POET3 mice exhibited enhanced growth and differentiation in organoid
13 cultures, as reflected by increased organoid number, larger organoid size and more distinct
14 differentiation of the CK8+ luminal layer and CK5+ basal layer within the organoids¹². To follow
15 the basal to luminal differentiation upon inflammation *in vivo* and verify the results from the *in*
16 *vitro* organoid cultures, we established a lineage tracing model, by crossing the POET3 mice
17 with the mTmG;KRT5-creERT2 mice in which the Tomato protein expressed in basal epithelial
18 cells switched to green fluorescent protein (GFP) upon the tamoxifen (Tmx)-induced *Krt5*
19 promoter-directed expression of Cre recombinase²¹. Lineage tracing was initiated in the
20 resulting transgenic colony (POET3^{het};mTmG^{het};KRT5-creERT2^{het}) with intraperitoneal injections
21 of Tmx, then activated OT-1 T cells were injected intravenously two weeks later to induce
22 inflammation in the prostates. Animals were euthanized a month after inflammation initiation for
23 both histological and flow cytometry analysis (Fig. 5C). Tmx injection induced GFP expression
24 in approximately 90% of prostate basal epithelial cells as demonstrated by immunofluorescent
25 staining with both anti-GFP and -CK5 antibodies (Supplemental Fig. 3A). Induction of GFP in
26 basal epithelial cells was also confirmed with flow cytometry (Supplemental Fig. 3B). To assess

1 the extent of basal to luminal differentiation after inflammation, prostate sections were stained
2 with antibodies against GFP, CK8 and CK5. GFP+ luminal cells were counted in anterior lobes.
3 We focused on anterior lobes because of their relative larger area, even under castrate
4 conditions as described later. Total number of GFP+ cells found within the CK8+ luminal layer
5 (GFP+CK8+) per mm² of acinar area was dramatically increased in inflamed prostates (Fig. 5E).
6 Increased number of GFP+ luminal cells in inflamed prostates was not only due to increased
7 basal to luminal differentiation, as reflected by the number of GFP+ foci in the luminal layer (Fig.
8 5F), but also due to increased proliferation of GFP+ cells after they differentiated into luminal
9 cells, as reflected by the number of cells within each GFP+ focus (Fig. 5G,H). Most (81%) GFP+
10 luminal cells found in naïve prostates were singles and the rest of the GFP+ luminal foci
11 contained at most two cells (Fig. 5G,I), whereas GFP+ luminal cells found in inflamed prostates
12 clustered in groups averaging 2.8 cells/cluster (Fig. 5G,H). 17% and 11% of GFP+ luminal foci
13 in inflamed prostates were found to contain 3-5 cells and over 6 cells, respectively (Fig. 5I).
14 Increased number of luminal GFP+ cells (identified as EpCAM+/CD49^{low}/GFP+) in inflamed
15 prostates were also confirmed with flow cytometry (Supplemental Fig. 3C). Of note, nearly all of
16 the GFP+ luminal cells expressed both luminal and basal markers (positive for both CK8 and
17 CK5) (Fig.5G) in both naïve and inflamed prostates, suggesting luminal cells derived from basal
18 stem cells retained basal features and were of a transitional phenotype, at least at the one-
19 month time point. Taken together, data collected from our lineage tracing model, together with
20 those from the BrdU incorporation experiment and organoid cultures, demonstrate that
21 inflammation promotes bPSC proliferation, their basal to luminal differentiation and proliferation
22 of the luminal epithelial cells.

23 Given that inflammation modulates AR level and activity in bPSC, we next examined
24 whether inflammation, by boosting AR signaling independent of androgen, is able to promote
25 bPSC expansion and their differentiation into luminal cells *in vivo* under castrate conditions.
26 Castration was performed two days after the initiation of inflammation so that the inflammation

1 was accompanied with reducing levels of androgen. BrdU incorporation was analyzed 7 days
2 after the initiation of inflammation and the presence of GFP+ luminal cells was analyzed one
3 month later (Fig. 5C). We first examined AR intensity and nuclear localization with
4 immunohistochemistry to confirm diminished AR activity after castration. AR nuclear staining in
5 the epithelial cells was found to be more intensified in inflamed prostates one week after the
6 initiation of inflammation compared to naïve prostates. A faint, diffuse cytoplasmic AR staining
7 pattern with little nuclear localization was observed in naïve prostates at merely five days after
8 castration, indicating a sharp reduction in circulating androgen, whereas the nuclear AR staining
9 persisted in inflamed prostates in castrated mice (Fig. 5D). Stronger cytoplasmic AR staining
10 was also observed in castrated inflamed prostates.

11 Inflammation-induced expansion of bPSC persisted with castration (Fig. 5B) and bPSC
12 proliferation as shown by BrdU incorporation remained significantly increased in inflamed
13 prostates even after castration (Fig. 5A), consistent with our previous findings that bPSC
14 population size in inflamed prostates remained unaffected with castration conducted two weeks
15 before inflammation¹². Interestingly, castration further increased the percentage of proliferating
16 bPSC in inflamed prostates, suggesting a synergistic effect of inflammation and androgen
17 deprivation on bPSC proliferation (Fig. 5A). Flow cytometry analysis of CD45+ leukocytes
18 infiltrated into the prostates confirmed that robust inflammation was induced under the castrate
19 condition (Supplemental Fig. 4). In our lineage tracing model, neither total number of GFP+
20 luminal cells or number of GFP+ foci was significantly altered with castration in inflamed
21 prostates (Fig. 5E,F). However, the size of GFP+ foci within the luminal layer in inflamed
22 prostates was significantly reduced with castration (Fig. 5H), with 88% of GFP+ luminal foci
23 containing only one cell, similar to naïve prostates (Fig. 5G,I). These data demonstrate that the
24 reduced level of androgen during inflammation does not affect the proliferation of bPSC, nor
25 does it affect their basal to luminal differentiation. However, normal levels of androgen are

1 essential for the proliferation of luminal cells during inflammation, as the transdifferentiated
2 GFP+ cells stopped growing into multi-cell clusters with castration.

3 In summary, we have demonstrated in a prostatitis model that AR activity is stimulated in
4 basal stem cells by inflammation and is essential for the luminal differentiation of these stem
5 cells. IL-1RA, which is strongly upregulated during inflammation, was identified for the first time
6 as the driver for AR activation independently of androgen in these stem cells and consequently
7 responsible for inflammation-induced differentiation (Fig. 6). Given the identical results from IL-
8 1RA or IL-1 α neutralizing Ab treatments, IL-1RA may trigger the downstream pathway that
9 leads to AR activation by antagonizing IL-1 α . Furthermore, we have demonstrated that
10 inflammation, by stimulating AR signaling in an androgen-independent fashion, promotes the
11 proliferation and differentiation of bPSC, even under castrate conditions.

12

13 **Discussion**

14 Although strong correlations have been reported between prostate inflammation and
15 BPH risk and progression¹⁻⁴, how inflammation contributes to the etiology of BPH remains
16 poorly understood. Data reported herein identify a novel mechanism, in which inflammation
17 drives the proliferation and differentiation of the stem cell population within the basal epithelial
18 layer, by inducing IL-1RA, which results in the enhancement of AR activation (Fig. 6). The
19 proposed mechanism was supported by data from both *in vitro* organoid cultures and an *in vivo*
20 lineage tracing model. Using organoid cultures for mechanistic studies, we have demonstrated
21 that IL-1RA is not only sufficient to induce AR activation independently of androgen and
22 promote differentiation in naïve bPSC-derived organoids, but also an essential mediator in
23 inflammation-driven AR activation, as inhibition of IL-1RA abrogated AR activation in inflamed
24 bPSC-derived organoids. In our lineage tracing model, inflammation greatly promoted the basal
25 to luminal differentiation even under castrate conditions by stimulating AR in bPSC

1 independently of androgen. Furthermore, we have demonstrated that by eliminating AR through
2 both pharmacological inhibition and genetic deletion, differentiation of bPSC into the luminal
3 lineage was significantly inhibited in organoid cultures, which corroborates a previous report on
4 the indispensable role of AR in the basal to luminal differentiation⁸ and further suggests that
5 inflammation is an important contributor to epithelial hyperplasia through the bPSC to luminal
6 differentiation process. Further studies are necessary to better understand the biological
7 implications of basal to luminal differentiation relative to homeostatic maintenance via luminal
8 progenitors^{9, 22}.

9 In our inflammation model, while castration did not impact inflammation-induced basal to
10 luminal differentiation, it inhibited the proliferation of differentiated luminal cells. Luminal GFP+
11 cells differentiated from the basal layer remained as single cells, in contrast to the multi-cell
12 luminal GFP+ clusters observed in non-castrate inflamed prostates. These data suggest that
13 inflammation may not affect AR activity in fibroblasts where AR activation induces fibroblast
14 secretion of growth factors such as NRG, IGF1 or FGF10. These growth factors bind to their
15 corresponding receptors on luminal epithelial cells and are critical for luminal proliferation and
16 replenishment during the prostate castration and regeneration cycle⁹ and in non-cell
17 autonomous prostate growth in sub-renal capsule simulated prostate growth²³. Under castrate
18 conditions, inflammation is not sufficient to sustain AR in fibroblasts and provide paracrine
19 signals for luminal proliferation.

20 IL-1RA exists as both a secreted form (sIL-1RA) and multiple intracellular non-secreted
21 forms^{24, 25}. The soluble extracellular sIL-1RA acts as an antagonist for IL-1R1 and competes
22 with IL-1 α or IL-1 β for IL-1R1 binding. The intracellular IL-1RAs have been shown to inhibit IL-
23 1R1-mediated target gene transcription but without affecting surface IL-1R1 engagement^{26, 27}.
24 Although IL-1RA (either the precursor of the soluble isoform or intracellular isoforms) could be
25 easily detected in the lysates of inflamed bPSC (Fig. 3D), consistent with the dramatic
26 upregulation of *Il1rn* transcripts with inflammation as revealed by our scRNA-seq analysis and

1 qRT-PCR, it is more likely that the extracellular soluble form mediates the effects of
2 inflammation. First of all, enhanced differentiation and AR activation observed in inflamed
3 organoids could be recapitulated in naïve organoids with the addition of recombinant IL-1RA in
4 the culture media. Conversely, the aforementioned phenotypes of inflamed organoids could be
5 reversed with the addition of a neutralizing antibody against IL-1RA. Secondly, the effects of
6 recombinant IL-1RA resemble those from an IL-1 α neutralizing antibody, suggesting that sIL-
7 1RA functions by antagonizing IL-1 α extracellularly and relieving IL-1 α 's suppression of AR
8 activity¹⁸⁻²⁰. IL-1R1 is likely to be the link connecting IL-1RA with the subsequent intracellular
9 events as our previous findings have demonstrated with a bacteria-induced prostate
10 inflammation model that inflammation-induced expansion of basal stem cell population was
11 significantly reduced in IL-1R1 knockout mice¹⁴. *In vivo* infiltrating leukocytes such as myeloid
12 cells in the inflamed prostates might also be the source for sIL-1RA^{28, 29}. The expression pattern
13 of IL-1RA in inflamed prostates, how IL-1RA from different sources contributes to stem cell AR
14 activation and differentiation, and other inflammatory factors³⁰⁻³² that may play critical functions
15 in AR stabilization during prostate hyperplasia are currently under investigation.

16 In contrast to the presence of AR in luminal prostate cells and some mature basal cells,
17 it has been reported by Xin *et al.* that only degraded AR was present in freshly isolated naïve
18 bPSC and in organoid cultures derived from them¹⁵. Our data have shown the presence of full-
19 length AR in the lysates from both inflamed bPSC and organoids, suggesting that inflammation
20 may promote the stabilization of AR (Fig. 1C,F). Inflammatory signals such as cytokines and
21 growth factors have been observed in the prostate cancer setting to stabilize AR independent of
22 androgen through phosphorylation events³³⁻³⁷. It is possible that IL-1RA may bind to IL-1R,
23 modulating NF κ B pathway members²⁰, altering the phosphorylation status of AR and ultimately
24 leading to AR stabilization. Understanding the mechanisms connecting inflammation, IL-1RA

1 and AR will potentially benefit the treatment of not only the benign prostate diseases such as
2 BPH but also malignant castration-resistant prostate cancer.

3 Taken together, our studies have identified IL-1RA as a novel AR modulator in the
4 inflamed prostate. IL-1RA is both sufficient and necessary for the stimulation of AR expression
5 and activity in bPSC and may be critical in inflammation-induced bPSC expansion and
6 differentiation and prostate hyperplasia.

1 **Methods**

2 **Animal studies**

3 Male mice aged 8-12 weeks were utilized for all studies. All animals were housed and
4 maintained under pathogen-free conditions with 12 hour-light/dark cycles. All procedures were
5 performed in accordance with protocols approved by Purdue University Animal Care and Use
6 Committee (PACUC). Mice were euthanized prior to harvest by CO₂ asphyxiation followed by
7 secondary cervical dislocation.

8 POET3 mice (C57BL/6 background) were generated as previous described¹⁰. Mice were
9 maintained in homozygous colonies. Inflammation was induced by adoptive transfer of 5x10⁶
10 pre-activated OT-1 cells (described below) via retro-orbital injection. Inflammation was allowed
11 to develop for 7 days before prostate harvest for bPSC analysis and organoid culture. For
12 inflammation/castration studies, mice were inflamed by adoptive transfer two days before
13 surgical orchiectomy. BrdU labeling and analysis were performed according to instructions
14 provided with APC BrdU Flow Kit (Becton Dickinson). Mice were injected with BrdU
15 intraperitoneally 2 hours before euthanasia.

16 OT-1 mice were purchased from Jackson Laboratories (Strain #:003831). As previously
17 described^{10, 12}, spleens from OT-1 mice were ground between frosted slides in RPMI-1640
18 medium (Gibco) with 10% fetal bovine serum (Corning). The resulting cell slurry was filtered
19 through a 70 µm cell strainer before treatment with Ammonium-Chloride-Potassium (ACK) lysis
20 buffer to remove red blood cells. Remaining splenocytes were re-suspended in RPMI-1640
21 medium and plated at 1x10⁶/well in 24-well plates with 1:1000 beta-mercaptoethanol (Gibco)
22 and 0.2 µg/mL SIINFEKL peptide (Ova peptide 257-264, AnaSpec). Cells were activated for 48
23 hours before purification using Ficoll (Cytiva) according to manufacturer's protocol.

24 For lineage tracing studies, POET3 mice were crossed with mTmG mice (Strain #:007676,
25 Jackson) and KRT5-CreERT2 mice (Strain #:029155, Jackson) to generate

1 POET3^{het};mTmG^{het};KRT5-creERT2^{het} mice that were used in the studies. To initiate lineage
2 tracing, mice were injected intraperitoneally with tamoxifen (Tmx) (Sigma-Aldrich) dissolved in
3 corn oil at the dosage of 3 mg/40 g (body weight) for four consecutive days. Inflammation was
4 induced via injection of pre-activated OT-1 T cells 2 weeks after Tmx injection and mice were
5 euthanized for analysis one month after inflammation.

6 Ar_flox/y mice strain was a generous gift from Dr. Robert E. Braun at The Jackson Laboratories.
7 AR deletion was achieved with Cre-GFP lentivirus (SignaGen Laboratories) infection. The
8 protocol of lentiviral infection was adopted and modified from Shahi *et al.*³⁸. Briefly, 10⁵ bPSC
9 isolated from Ar_flox/y mice were mixed with 100 µL lentivirus and 4 µg/mL polybrene and
10 centrifuged at 1,800 rpm for 90 minutes. Cells were washed once with DMEM media (Gibco)
11 and re-suspended for organoid culture as described below.

12 Orchiectomy: Mice were anesthetized using isoflurane gas. After thorough cleaning of the
13 surgical area, a small incision was made at the base of the scrotum. Another, smaller incision
14 was made in the inner membrane surrounding the testicle, which was pushed out by gentle
15 pressure on the abdomen. Once extracted, the connective tissue and blood vessels were
16 cauterized with heated forceps before cutting. This was repeated for the second testicle. The
17 incisions were sutured shut. Flunixin and Bupivacaine were administered as analgesics.

18 **Isolation of bPSC population**

19 This process was a modification of a well-established protocol^{12, 39}. Briefly, minced prostate
20 tissues were digested in 1 mg/mL collagenase (Sigma-Aldrich) in RPMI-1640 (Gibco) media
21 containing 10% FBS (Corning) with shaking at 37°C for 2 hours, followed by trypsinization.
22 Dissociated cells were passed through 20G needles and 40 µm cell strainers to eliminate
23 aggregates, followed by removal of red blood cells by ACK buffer. To enrich murine bPSC,
24 isolated cells were stained with Zombie Violet Live/Dead Fixable Viability Dye (Biolegend) in
25 PBS, followed by incubation with 1:100 diluted fluorescence-conjugated specific antibodies
26 (Biolegend): CD45-FITC (#103108), CD31-FITC (#102506), Sca-1-APC (#122512) and CD49f-

1 PE (#313612). Human prostate samples from unidentified patients were acquired from Indiana
2 University School of Medicine Tissue Repository under IRB-approved protocols. Isolated human
3 prostate cells were stained with Zombie UV Fixable Viability Dye (Biolegend), CD45-FITC
4 (#304006), EpCAM-PE (#324206), CD26-APC (#302710) and CD49f-BV421 (#313624) as
5 described in detail by Strand *et al.*⁴⁰. Once stained, fluorescence activated cell sorting was
6 performed on the BD FACSAria under sterile conditions.

7 **Organoid culture**

8 Organoid culture protocol was adapted from Lukacs *et al.*³⁹. Briefly, sorted bPSC were counted
9 and resuspended in a 1:2 mixture of Prostate Epithelial Growth Medium (PrEGM, Lonza) and
10 Matrigel (growth factor reduced, Corning). The mixture was deposited in a ring around the edge
11 of a refrigerated 12-well plate at 10⁴ cells/120 μ L/well and allowed to solidify for 15 minutes at
12 37°C before addition of pre-warmed PrEGM with or without treatments. Growth medium with
13 treatments was changed every 2-3 days before counting and harvesting on day 7. The following
14 treatments were used with vehicle controls: Enzalutamide (Selleckchem), R1881 (Sigma-
15 Aldrich), recombinant mouse IL-1RA (R&D Systems), recombinant mouse IL-1 α (R&D), IL1-RA
16 neutralizing antibody (#AF-480-NA, R&D) and IL-1 α neutralizing antibody (#AF-400-NA, R&D).
17 Intact organoids were released from Matrigel with Dispase (Gibco), fixed in 10% neutral
18 buffered formalin followed by 70% ethanol, and embedded in HistoGel (ThermoFisher
19 Scientific).

20 **AR target gene PCR array**

21 Total RNA was isolated from freshly sorted bPSC or organoids using TRIzol Reagent
22 (Invitrogen) according to manufacturer's protocol. cDNA was synthesized using M-MuLV
23 Reverse Transcriptase (New England Biolabs). Global AR target gene array analysis was
24 conducted with Qiagen RT2 Profiler PCR Array-Mouse Androgen Receptor Signaling Targets
25 (#PAMM-142ZF) and Qiagen online data analyzer. Differentially expressed genes in both naïve

1 and inflamed groups (threshold cycle <35) were further subjected to statistical analysis, where
2 the significance was determined by $\alpha=0.05$.

3 **Quantitative real-time polymerase chain reaction**

4 Quantitative real-time polymerase chain reaction (qRT-PCR) was conducted using PerfeCTa
5 qPCR FastMix II (QuantaBio) together with 6-FAM/ZEN/IBFQ primer/probe sets (PrimeTime
6 qPCR Assays, IDT) and VIC-labeled TaqMan Ribosomal RNA Control Reagents (Applied
7 Biosystems) on Roche LightCycler 96 according to manufacturers' protocols. Triplicate samples
8 from three independent mice were analyzed for each group. Relative gene expression was
9 calculated using the formula $2^{-[Ct(\text{target gene})-Ct(18S)]}$ where Ct refers to the cycle threshold.

10 **Western blot**

11 Protein was isolated from freshly sorted bPSC or organoids using TRIzol Reagent (Invitrogen)
12 according to manufacturer's protocol and 30-50 μg protein lysates were used. AR protein was
13 detected using rabbit anti-AR (N-20) antibody (#sc-816, Santa Cruz Biotechnology) at 1:200
14 dilution followed by IRDye 680RD goat anti-rabbit IgG antibody (Li-Cor) at 1:10,000 dilution. The
15 blot was then incubated with mouse anti- β -Actin or mouse anti-Vinculin antibody (Sigma-
16 Aldrich) followed by IRDye 800CW goat anti-mouse antibody (Li-Cor). Blots were imaged using
17 Odyssey CLx Infrared Imaging system (Li-Cor).

18 **ELISA**

19 Protein was isolated from freshly sorted bPSC using TRIzol Reagent (Invitrogen). IL-1RA and
20 IL-1 α in bPSC lysates were detected using Mouse IL-1ra/IL-1F3 Quantikine ELISA Kit and
21 Mouse IL-1 alpha/IL-1F1 Quantikine ELISA Kit (R&D), respectively, according to manufacturer's
22 instructions.

23 **Flow cytometry analysis**

24 Protocols were adopted from our previous study¹². Prostate tissues were processed as
25 described above for bPSC isolation and isolated cells were stained with the following

1 fluorescence conjugated antibodies (Biolegend): CD45-PerCP (#103130), Sca-1-APC
2 (#122512) and CD49f-PE (#313612) before fixation with 10% neutral buffered formalin. To
3 detect AR protein, fixed samples were stained with unconjugated rabbit anti-AR (#ab52615,
4 Abcam, 1:50) followed by secondary stain with Alexa Fluor 488 (Invitrogen, 1:500). Prostate
5 cells isolated from lineage tracing mice were stained with the following fluorescence conjugated
6 antibodies (Biolegend): EpCAM-PE/Cyanine7 (#18215) and CD49f-BV421(#313623). Flow
7 cytometry analyses were performed using BD LSRFortessa.

8 **Histology**

9 Formalin fixed samples were paraffin embedded and sectioned at 4 μm onto charged
10 microscope slides. Tissues were deparaffinized through multiple changes of Xylene and 100%
11 Ethanol. Immunohistochemistry: Anti-AR antibody (#ab133273, Abcam) was applied at 1:500
12 dilution for 30 minutes and the secondary antibody ImmPRESS HRP Goat anti-Rabbit (#MP-
13 7451-50, Novus Biologicals) was also applied for 30 minutes. Following this, the DAB
14 chromogen was applied for 5 minutes. Slides were double rinsed with Tris buffer between all
15 steps. Slides were counterstained with hematoxylin before covered with resinous mounting
16 media. Immunofluorescence: The primary GFP antibody (#A-11122, Invitrogen) was applied at
17 a 1:250 dilution for 30 minutes followed by incubation with a secondary Goat anti-Rabbit
18 antibody conjugated with Alexa Fluor 647 (Invitrogen). Slides were blocked twice again with
19 2.5% normal rabbit serum followed by AffiniPure Fab Goat anti-Rabbit (#111-007-003, Jackson
20 ImmunoResearch Laboratories) at 20 $\mu\text{g}/\text{mL}$. Primary antibodies anti-CK5 (1:500) (#905501,
21 Biolegend) and anti-CK8 (1:1000) (#904804, Biolegend) were applied for 60 minutes. The
22 secondary antibodies Goat anti-Rabbit conjugated with Dylight 488 and Goat anti-Mouse
23 conjugated with Alexa Fluor 555 (Invitrogen) were applied for 30 minutes. Slides received a
24 DAPI counterstain at 1 $\mu\text{g}/\text{mL}$ for 10 minutes and were covered with ProLong Gold Antifade
25 Mountant (Invitrogen). Slide digitization was conducted on the Leica Aperio VERSA 8 Whole

1 Slide Scanner in the appropriate brightfield and fluorescent settings. Digital images were
2 uploaded to eSlide Manager for analysis. For AR immunofluorescent staining, sections were
3 incubated with the indicated primary antibodies overnight at 4°C: rat anti-AR (#MA1-150,
4 Invitrogen, 4 µg/mL) or rabbit anti-AR (#PA5-16363, Invitrogen, 2 µg/mL). Species-specific
5 Alexa 488 and Alexa 594-conjugated secondary antibodies (Invitrogen) were applied for 1 hour
6 at room temperature at a dilution of 1:200. Nuclei were stained by incubation with Hoechst
7 33258 nuclear stain (Sigma-Aldrich) at a concentration of 1 µg/mL. All specimens were
8 visualized using immunofluorescence intensity with the Leica 6000 epifluorescence/confocal
9 microscope.

10 **Single Cell RNA Sequencing**

11 Data was collected at the Purdue Cell Cytometry Facility using the C1 Fluidigm instrument with
12 SMARTer chemistry (Clontech) to generate cDNA from captured single cells. The Purdue
13 Genomics Facility prepared libraries using a Nextera kit (Illumina). Single-end 1x50 bp reads
14 were sequenced using the HiSeq2500 on rapid run mode. FastX-Toolkit v. 0.0.13.2 (Gordon, A.,
15 FastX-Toolkit. 2009) quality trimmer was used to further trim reads based on quality score and
16 FASTX-Toolkit quality chart was used to make read per-base quality plots. A trimscore and a
17 trim length of 30 were used. Tophat2 was used to align reads to the *Mus musculus* GRCm38.p6
18 reference genome^{41, 42}. Tophat2 was run with defaults except that the number of mismatches
19 allowed was 1. The htseq-count script in HTSeq v.0.6.1⁴³ and Biopython v.2.7.3 were used to
20 generate a counts matrix in “intersection-nonempty” mode, with feature set to “exon” and
21 attribute parameter set to “gene_id”. R version R-3.4.1 and the package Seurat v. 1.4 was used
22 to cluster cells into subpopulations⁴⁴ using the first 4 principal components, a resolution of 0.5,
23 and k.param = 4. The FindAllMarkers() function within Seurat was used to identify cluster
24 markers using the zero-inflated “bimod” model and a false discovery rate (FDR) of 0.01.
25 FindAllMarkers() was likewise used to identify differentially expressed genes between inflamed

1 and naïve cells, controlling the FDR at 5%. Ingenuity Pathway Analysis (IPA, Qiagen) was used
2 to perform pathway analyses and enrichment analyses.

3 **Statistical Analysis**

4 Statistical analyses were performed using GraphPad Prism (v.9.5.1). Two-tailed unpaired
5 Student's t-test or Welch's t test was performed for comparisons between two groups. Unpaired
6 ordinary one-way analysis of variance (ANOVA), or Brown-Forsythe and Welch ANOVA tests,
7 followed by multiple comparisons was performed for comparisons among three or more groups.
8 *P* values less than 0.05 are considered as significant. Data are presented as means \pm SEM
9 (standard error of mean).

10

1 **Data availability**

- 2 The authors declare that all data supporting the findings of this study are available within the
3 paper (and its supplementary information files).

1 **Acknowledgements:**

2 We thank Dr. Jill Hutchcroft at Purdue Flow Cytometry & Cell Separation Facility for cell sorting;
3 Histology Research Laboratory at Purdue College of Veterinary Medicine, a core facility of the
4 NIH-funded Indiana Clinical and Translational Science Institute, for histology processing,
5 immunohistochemistry and immunofluorescence staining. This project was supported by NIDDK
6 2R01DK084454 and Purdue Institute for Cancer Research P30CA023168. This project was also
7 funded with support from the Indiana Clinical and Translational Sciences Institute which is
8 funded in part by Award Number UM1TR004402 from the National Institutes of Health, National
9 Center for Advancing Translational Sciences, Clinical and Translational Sciences Award. The
10 content is solely the responsibility of the authors and does not necessarily represent the official
11 views of the National Institutes of Health.

12

1 **Author contributions**

2 T.L.R., T.J.J., J.Y., and P.O.C designed the study and interpreted the data. J.Y., P.O.C and
3 T.L.R. wrote the manuscript. P.O.C., J.Y., H-H.W., M.M.B., G.D.A., G.M.C. and L.W. carried out
4 the experiments. E.G., N.A.L., R.W.D. and F.Z. analyzed the scRNA-seq data. *Ar_flox/y* mice
5 were provided by R.E.B. and lineage tracing mice were generated by J.Y. and P.O.C.. L.C.
6 provided histological analyses and S.A.C. participated in study design and data interpretation.

7

1 **References**

- 2 1. Gandaglia, G. *et al.* The role of prostatic inflammation in the development and
3 progression of benign and malignant diseases. *Curr Opin Urol* **27**, 99-106 (2017).
- 4 2. De Nunzio, C., Presicce, F. & Tubaro, A. Inflammatory mediators in the development
5 and progression of benign prostatic hyperplasia. *Nat Rev Urol* **13**, 613-626 (2016).
- 6 3. Nickel, J.C. *et al.* The relationship between prostate inflammation and lower urinary tract
7 symptoms: examination of baseline data from the REDUCE trial. *Eur Urol* **54**, 1379-1384
8 (2008).
- 9 4. Robert, G. *et al.* Inflammation in benign prostatic hyperplasia: a 282 patients'
10 immunohistochemical analysis. *Prostate* **69**, 1774-1780 (2009).
- 11 5. Lawson, D.A. *et al.* Basal epithelial stem cells are efficient targets for prostate cancer
12 initiation. *Proc Natl Acad Sci U S A* **107**, 2610-2615 (2010).
- 13 6. Crowell, P.D. *et al.* Expansion of Luminal Progenitor Cells in the Aging Mouse and
14 Human Prostate. *Cell Rep* **28**, 1499-1510 e1496 (2019).
- 15 7. Toivanen, R., Mohan, A. & Shen, M.M. Basal Progenitors Contribute to Repair of the
16 Prostate Epithelium Following Induced Luminal Anoikis. *Stem Cell Reports* **6**, 660-667
17 (2016).
- 18 8. Xie, Q. *et al.* Dissecting cell-type-specific roles of androgen receptor in prostate
19 homeostasis and regeneration through lineage tracing. *Nat Commun* **8**, 14284 (2017).
- 20 9. Karthaus, W.R. *et al.* Regenerative potential of prostate luminal cells revealed by single-
21 cell analysis. *Science* **368**, 497-505 (2020).
- 22 10. Haverkamp, J.M. *et al.* An inducible model of abacterial prostatitis induces antigen
23 specific inflammatory and proliferative changes in the murine prostate. *Prostate* **71**,
24 1139-1150 (2011).

- 1 11. Kwon, O.J., Zhang, L. & Xin, L. Stem Cell Antigen-1 Identifies a Distinct Androgen-
2 Independent Murine Prostatic Luminal Cell Lineage with Bipotent Potential. *Stem Cells*
3 **34**, 191-202 (2016).
- 4 12. Wang, H.H. *et al.* Characterization of autoimmune inflammation induced prostate stem
5 cell expansion. *Prostate* **75**, 1620-1631 (2015).
- 6 13. Kwon, O.J., Zhang, L., Ittmann, M.M. & Xin, L. Prostatic inflammation enhances basal-
7 to-luminal differentiation and accelerates initiation of prostate cancer with a basal cell
8 origin. *Proc Natl Acad Sci U S A* **111**, E592-600 (2014).
- 9 14. Wang, L. *et al.* Expansion of prostate epithelial progenitor cells after inflammation of the
10 mouse prostate. *Am J Physiol Renal Physiol* **308**, F1421-1430 (2015).
- 11 15. Xin, L., Lukacs, R.U., Lawson, D.A., Cheng, D. & Witte, O.N. Self-renewal and
12 multilineage differentiation in vitro from murine prostate stem cells. *Stem Cells* **25**, 2760-
13 2769 (2007).
- 14 16. Henry, G.H. *et al.* A Cellular Anatomy of the Normal Adult Human Prostate and Prostatic
15 Urethra. *Cell Rep* **25**, 3530-3542 e3535 (2018).
- 16 17. Culig, Z. *et al.* Interleukin 1beta mediates the modulatory effects of monocytes on
17 LNCaP human prostate cancer cells. *Br J Cancer* **78**, 1004-1011 (1998).
- 18 18. Staverosky, J.A., Zhu, X.H., Ha, S. & Logan, S.K. Anti-androgen resistance in prostate
19 cancer cells chronically induced by interleukin-1beta. *Am J Clin Exp Urol* **1**, 53-65
20 (2013).
- 21 19. Chang, M.A. *et al.* IL-1beta induces p62/SQSTM1 and represses androgen receptor
22 expression in prostate cancer cells. *J Cell Biochem* **115**, 2188-2197 (2014).
- 23 20. Thomas-Jardin, S.E. *et al.* RELA is sufficient to mediate interleukin-1 repression of
24 androgen receptor expression and activity in an LNCaP disease progression model.
25 *Prostate* **80**, 133-145 (2020).

- 1 21. Muzumdar, M.D., Tasic, B., Miyamichi, K., Li, L. & Luo, L. A global double-fluorescent
2 Cre reporter mouse. *Genesis* **45**, 593-605 (2007).
- 3 22. Crowley, L. & Shen, M.M. Heterogeneity and complexity of the prostate epithelium: New
4 findings from single-cell RNA sequencing studies. *Cancer Lett* **525**, 108-114 (2022).
- 5 23. Zhang, B. *et al.* Non-Cell-Autonomous Regulation of Prostate Epithelial Homeostasis by
6 Androgen Receptor. *Mol Cell* **63**, 976-989 (2016).
- 7 24. Gabay, C., Porter, B., Fantuzzi, G. & Arend, W.P. Mouse IL-1 receptor antagonist
8 isoforms: complementary DNA cloning and protein expression of intracellular isoform
9 and tissue distribution of secreted and intracellular IL-1 receptor antagonist in vivo. *J*
10 *Immunol* **159**, 5905-5913 (1997).
- 11 25. Martin, P. *et al.* Intracellular IL-1 Receptor Antagonist Isoform 1 Released from
12 Keratinocytes upon Cell Death Acts as an Inhibitor for the Alarmin IL-1alpha. *J Immunol*
13 **204**, 967-979 (2020).
- 14 26. Watson, J.M. *et al.* The intracellular IL-1 receptor antagonist alters IL-1-inducible gene
15 expression without blocking exogenous signaling by IL-1 beta. *J Immunol* **155**, 4467-
16 4475 (1995).
- 17 27. Vecile, E. *et al.* Intracellular function of interleukin-1 receptor antagonist in ischemic
18 cardiomyocytes. *PLoS One* **8**, e53265 (2013).
- 19 28. Giavridis, T. *et al.* CAR T cell-induced cytokine release syndrome is mediated by
20 macrophages and abated by IL-1 blockade. *Nat Med* **24**, 731-738 (2018).
- 21 29. Gander-Bui, H.T.T. *et al.* Targeted removal of macrophage-secreted interleukin-1
22 receptor antagonist protects against lethal *Candida albicans* sepsis. *Immunity* **56**, 1743-
23 1760 e1749 (2023).
- 24 30. Lee, S.O., Lou, W., Hou, M., Onate, S.A. & Gao, A.C. Interleukin-4 enhances prostate-
25 specific antigen expression by activation of the androgen receptor and Akt pathway.
26 *Oncogene* **22**, 7981-7988 (2003).

- 1 31. Hobisch, A. *et al.* Interleukin-6 regulates prostate-specific protein expression in prostate
2 carcinoma cells by activation of the androgen receptor. *Cancer Res* **58**, 4640-4645
3 (1998).
- 4 32. Culig, Z. *et al.* Androgen receptor activation in prostatic tumor cell lines by insulin-like
5 growth factor-I, keratinocyte growth factor, and epidermal growth factor. *Cancer Res* **54**,
6 5474-5478 (1994).
- 7 33. Koryakina, Y., Ta, H.Q. & Gioeli, D. Androgen receptor phosphorylation: biological
8 context and functional consequences. *Endocr Relat Cancer* **21**, T131-145 (2014).
- 9 34. Willder, J.M. *et al.* Androgen receptor phosphorylation at serine 515 by Cdk1 predicts
10 biochemical relapse in prostate cancer patients. *Br J Cancer* **108**, 139-148 (2013).
- 11 35. Ponguta, L.A., Gregory, C.W., French, F.S. & Wilson, E.M. Site-specific androgen
12 receptor serine phosphorylation linked to epidermal growth factor-dependent growth of
13 castration-recurrent prostate cancer. *J Biol Chem* **283**, 20989-21001 (2008).
- 14 36. Guo, Z. *et al.* Regulation of androgen receptor activity by tyrosine phosphorylation.
15 *Cancer Cell* **10**, 309-319 (2006).
- 16 37. Gioeli, D. *et al.* Androgen receptor phosphorylation. Regulation and identification of the
17 phosphorylation sites. *J Biol Chem* **277**, 29304-29314 (2002).
- 18 38. Shahi, P., Seethammagari, M.R., Valdez, J.M., Xin, L. & Spencer, D.M. Wnt and Notch
19 pathways have interrelated opposing roles on prostate progenitor cell proliferation and
20 differentiation. *Stem Cells* **29**, 678-688 (2011).
- 21 39. Lukacs, R.U., Goldstein, A.S., Lawson, D.A., Cheng, D. & Witte, O.N. Isolation,
22 cultivation and characterization of adult murine prostate stem cells. *Nat Protoc* **5**, 702-
23 713 (2010).
- 24 40. Strand, D.W., Aaron, L., Henry, G., Franco, O.E. & Hayward, S.W. Isolation and analysis
25 of discreet human prostate cellular populations. *Differentiation* **91**, 139-151 (2016).

- 1 41. Trapnell, C., Pachter, L. & Salzberg, S.L. TopHat: discovering splice junctions with RNA-
2 Seq. *Bioinformatics* **25**, 1105-1111 (2009).
- 3 42. Kim, D. *et al.* TopHat2: accurate alignment of transcriptomes in the presence of
4 insertions, deletions and gene fusions. *Genome Biol* **14**, R36 (2013).
- 5 43. Anders, S., Pyl, P.T. & Huber, W. HTSeq--a Python framework to work with high-
6 throughput sequencing data. *Bioinformatics* **31**, 166-169 (2015).
- 7 44. Satija, R., Farrell, J.A., Gennert, D., Schier, A.F. & Regev, A. Spatial reconstruction of
8 single-cell gene expression data. *Nat Biotechnol* **33**, 495-502 (2015).
- 9

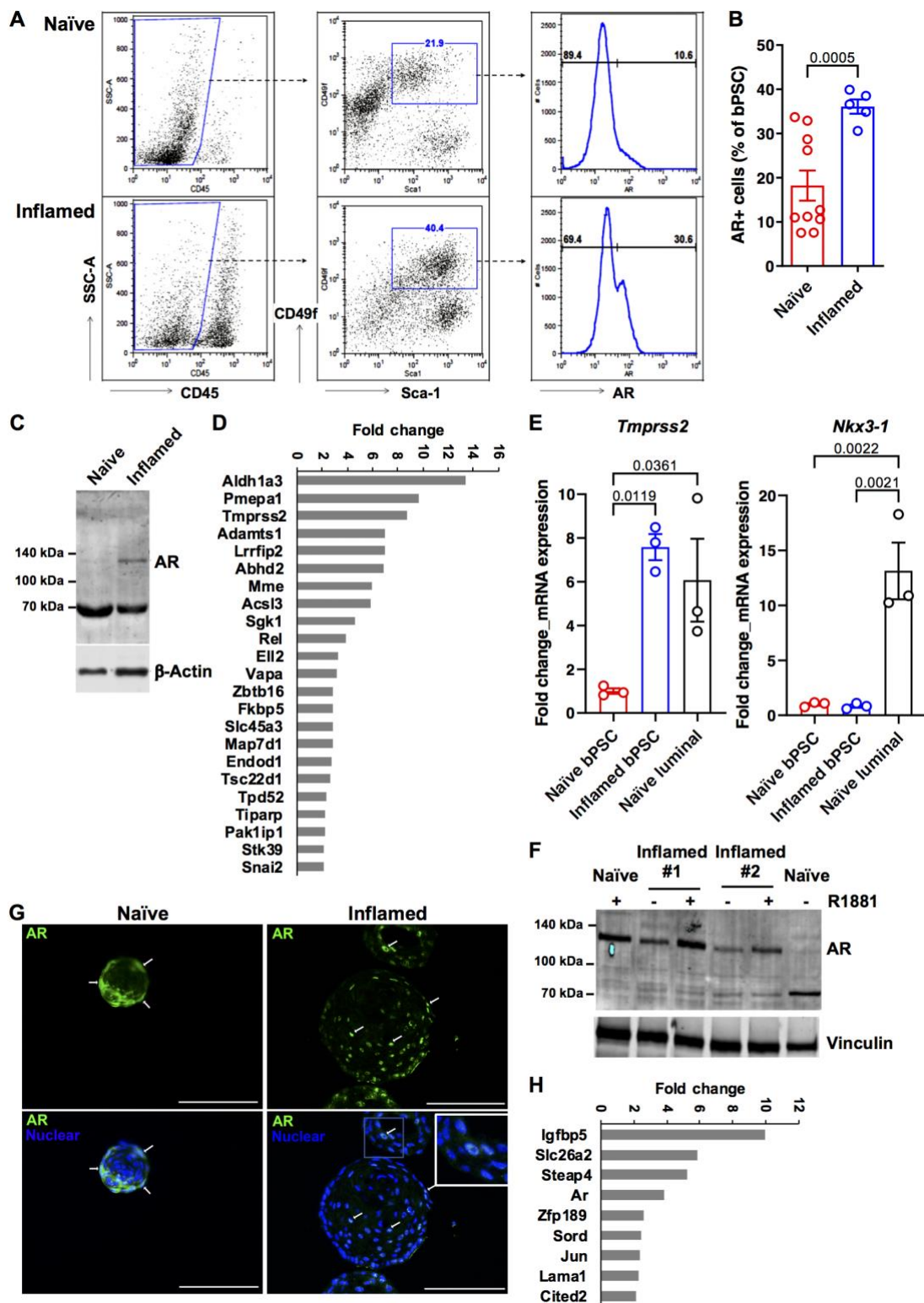


Figure 1. AR expression and activity are elevated in bPSC freshly isolated from inflamed prostates and the enhanced AR activity was sustained in inflamed organoids in the absence of androgen. (A) Representative flow cytometry dot plots and histograms of intracellular AR in bPSC from naïve and inflamed prostates. **(B)** Bar graph showing the percentage of AR+ cells within naïve and inflamed bPSC population as analyzed with flow cytometry (Naïve, n=10; Inflamed, n=5). **(C)** Immunoblot of full-length AR in naïve and inflamed bPSC lysates. **(D)** Fold change of AR target genes significantly upregulated in inflamed bPSC (Naïve or Inflamed, n=3). **(E)** qRT-PCR of conventional AR target genes, *Tmprss2* and *Nkx3-1*, in bPSC. Matched luminal population is included as a control (Naïve or Inflamed, n=3). **(F)** Immunoblot showing increased level of full-length AR in inflamed organoids compared to naïve organoids. Full-length AR levels in both naïve and inflamed organoids were elevated with 1 nM R1881 treatment. **(G)** AR Immunofluorescence staining in organoids derived from naïve or inflamed bPSC. Representative cells with nuclear localized AR are indicated with white arrows AR nuclear localization is also shown in the inset image with higher magnification (Scale bar, 100 μ m). **(H)** Fold change of AR target genes significantly upregulated in inflamed organoids (Naïve or Inflamed, n=3).

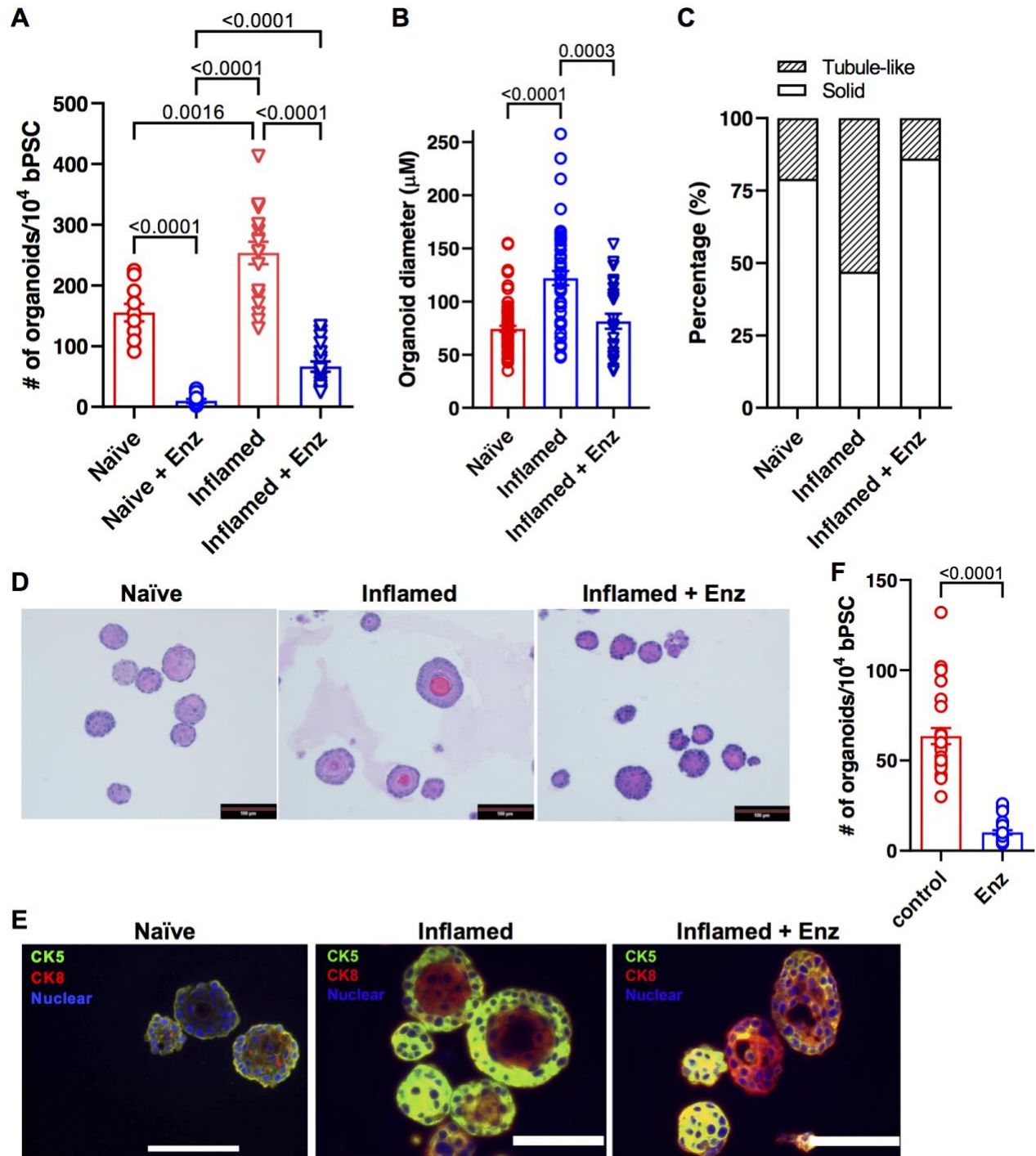


Figure 2. Abrogation of AR activity inhibits the differentiation of inflamed bPSC in organoid cultures. (A) Number of organoids formed with naïve, inflamed bPSC with or without 10 μ M Enz treatment (Naïve groups, n=10; Inflamed groups, n=18). **(B)** Diameter of organoids and **(C)** percentage of organoids with tubule-like structures in naïve, inflamed organoids or inflamed organoids treated with Enz (Naïve, n=74; Inflamed, n=47; Inflamed+Enz, n=25). **(D)** Representative H&E images of naïve, inflamed organoids or inflamed organoids treated with Enz (Scale bar, 100 μ m). **(E)** CK5 (green) and CK8 (red) staining showing lack of organization in Enz-treated inflamed organoids (Scale bar, 25 μ m). **(F)** Enz significantly reduces the number of organoids formed with human PSC (control or Enz, n=27).

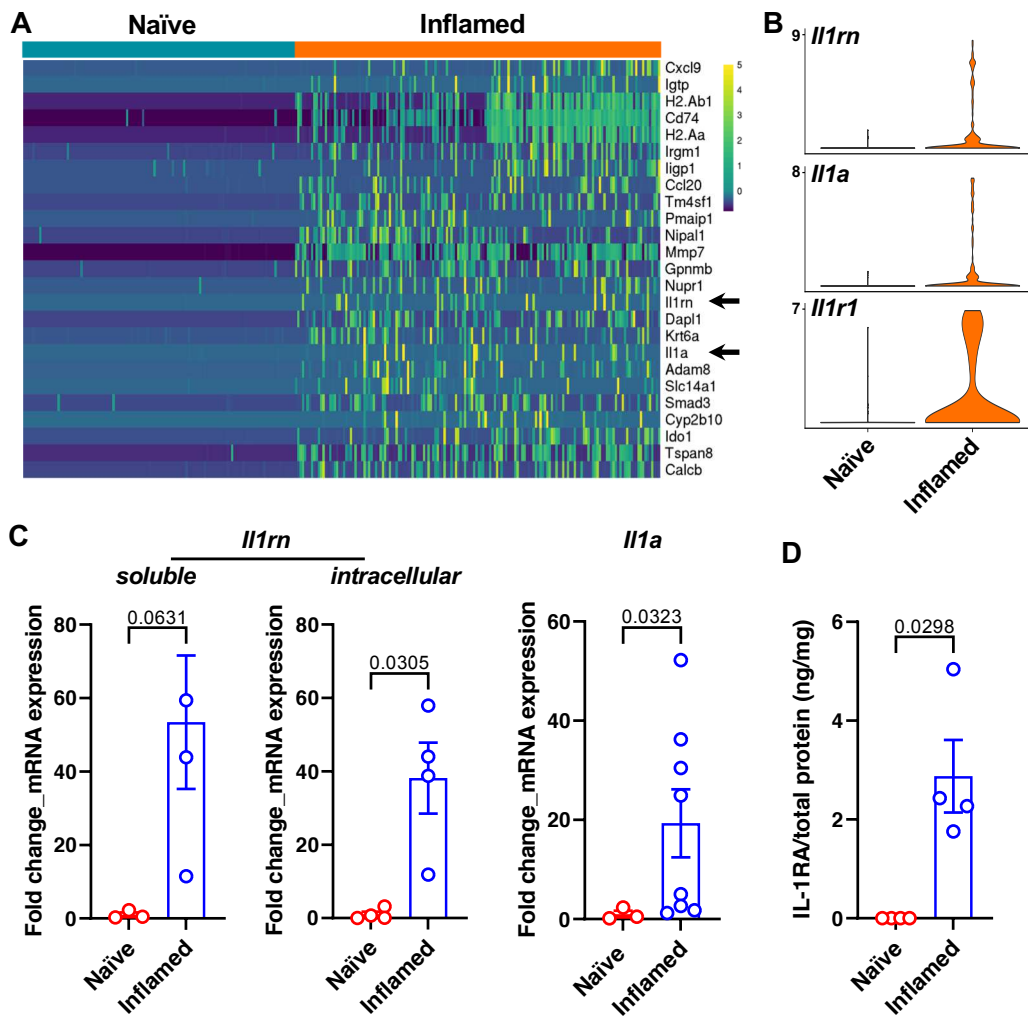


Figure 3. IL-1RA is upregulated in inflamed bPSC. (A) *Il1rn* and *Il1a* (arrows) are among the most upregulated genes in the inflamed bPSC compared to naïve bPSC as analyzed with scRNA-seq. (B) Violin plots of *Il1rn*, *Il1a* and *Il1r1* expression in naïve and inflamed bPSC. (C) qRT-PCR of *Il1rn* isoforms and *Il1a* in naïve and inflamed bPSC (Naïve, n=3-4; Inflamed, n=3-8). (D) Upregulation of IL-1RA protein is confirmed using ELISA with lysates collected from naïve or inflamed bPSC (Naïve or Inflamed, n=4).

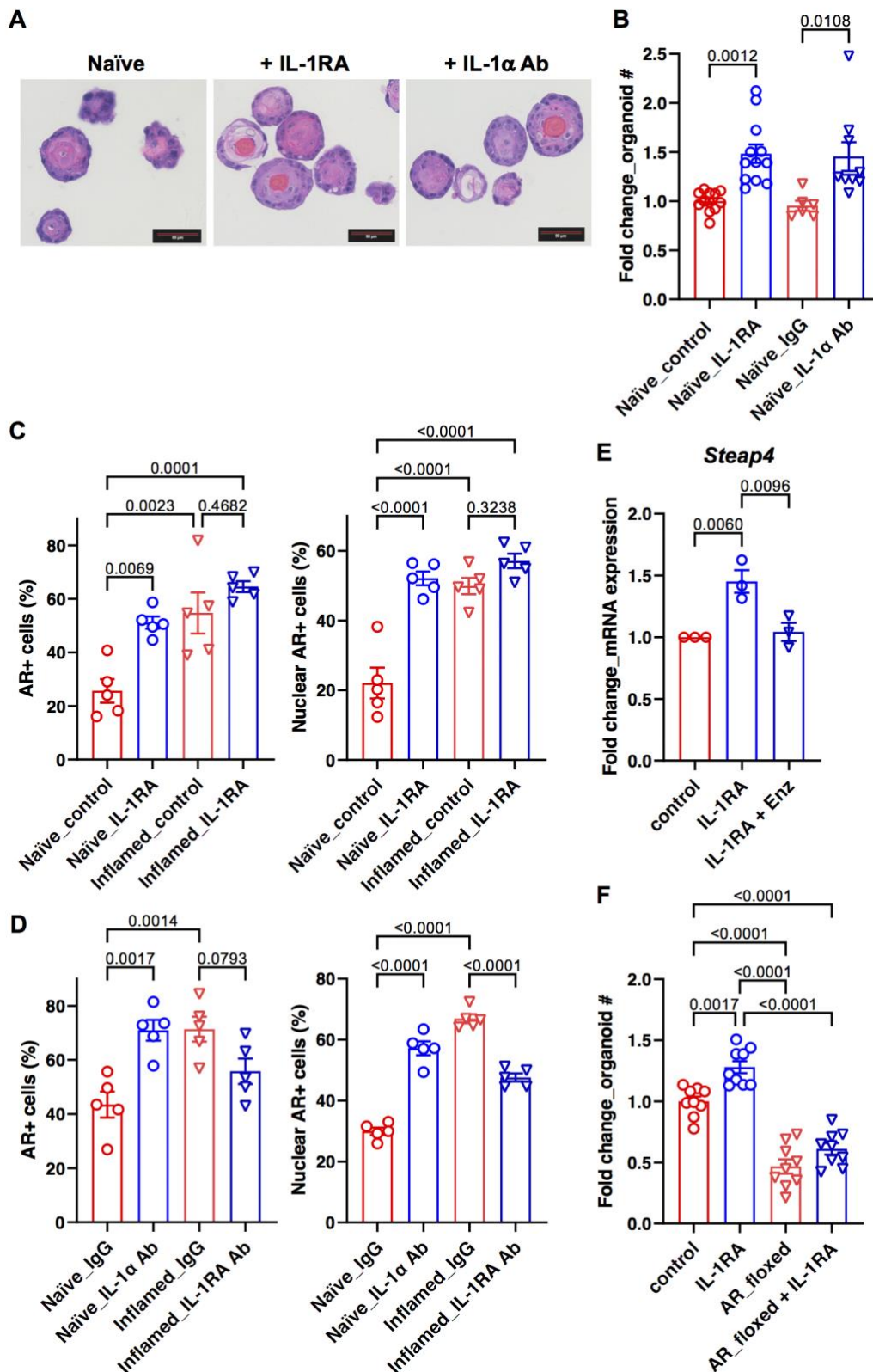


Figure 4. IL-1RA mediates inflammation-induced differentiation and AR activity in bPSC organoids. (A) Representative H&E images of naïve organoids treated with recombinant IL-1RA or neutralizing antibody (Ab) against IL-1 α , showing an increase in stratification of treated organoids (Scale bar, 50 μ m). (B) Organoid formation with naïve bPSC was significantly increased with recombinant IL-1RA (50 ng/mL) or IL-1 α neutralizing Ab treatment (5 μ g/mL) (Naïve_control, n=12; Naïve_IL-1RA, n=12; Naïve_IgG, n=6; Naïve_IL-1 α Ab, n=9). (C) Quantitation of AR+ (both overall and nuclear) cells in naïve or inflamed organoids treated with IL-1RA (50 ng/mL) (All groups, n=5). (D) AR staining (overall and nuclear) was increased in naïve organoids treated with an IL-1 α neutralizing Ab (5 μ g/mL) and decreased in inflamed organoids treated with an IL-1RA neutralizing Ab (5 μ g/mL) (All groups, n=5). (E) qRT-PCR showing the AR target gene *Steap4* was upregulated with IL-1RA in naïve organoids and Enz treatment abolished the upregulation (All groups, n=3). (F) The effects of IL-1RA were lost with naïve organoids derived from *Ar_flox/y* bPSC which were deprived of AR (All groups, n=9).

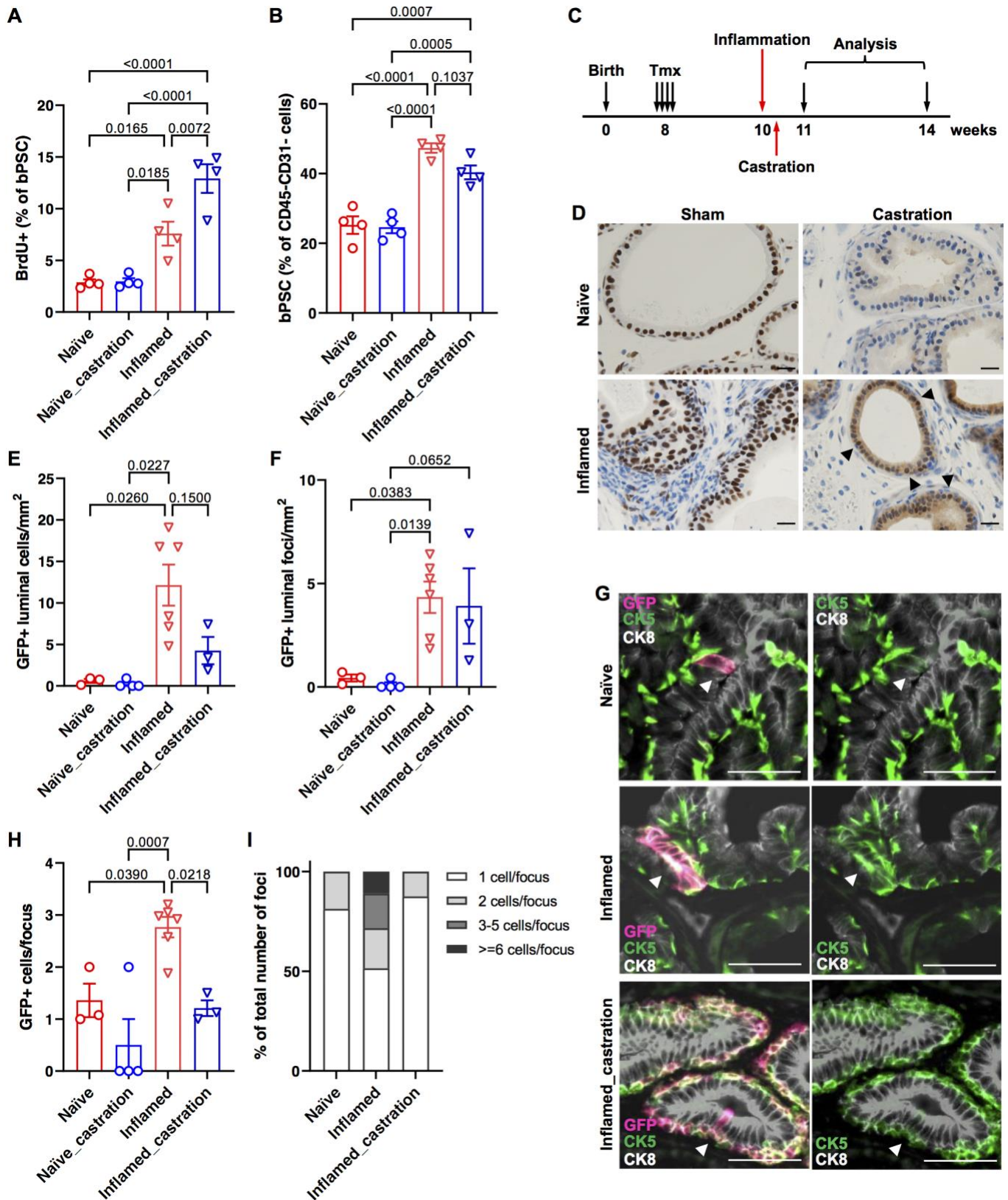


Figure 5. Inflammation mimicking non-bacterial prostatitis promotes the proliferation of basal stem cells and the basal to luminal differentiation *in vivo*. (A) Quantitation of BrdU+ bPSC in naïve and inflamed prostates, with or without castration (All groups, n=4). (B) Percentage of bPSC in naïve and inflamed prostates, with or without castration (All groups, n=4). (C) Experimental scheme showing time points of inflammation, castration and analysis. (D) AR staining shows maintenance of AR nuclear localization (arrow heads) in castrated inflamed prostates (Scale bar, 20 μ m). (E,F) Quantitation of GFP+ cells or foci within the luminal layer (Naïve, n=3; Naïve_castration, n=4; Inflamed, n=6; Inflamed_castration, n=3). (G) Representative immunofluorescent images from naïve and inflamed prostates with or without castration showing the presence of GFP+CK5+ cells within the CK8+ luminal layer (arrowheads) (Scale bar, 50 μ m). (H,I) Size of GFP+ foci and percentage of GFP+ foci of different sizes within the luminal layer (Naïve, n=3; Naïve_castration, n=4; Inflamed, n=6; Inflamed_castration, n=3).

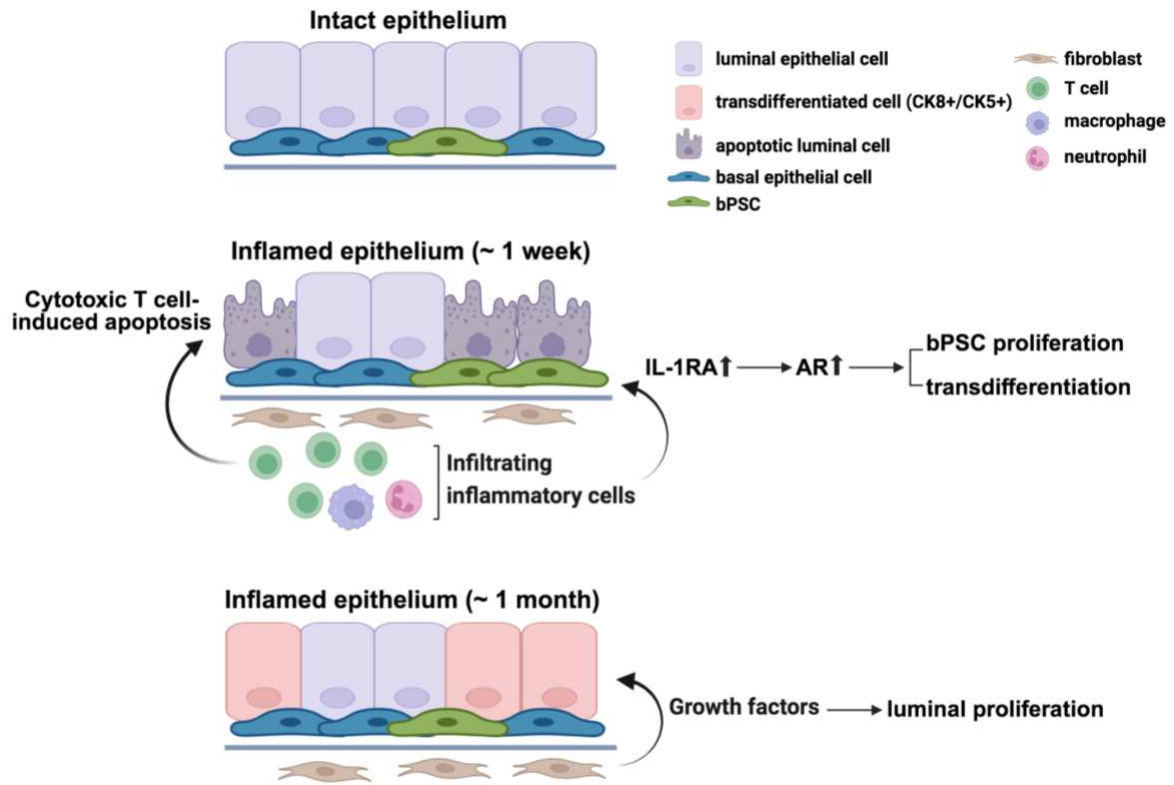


Figure 6. Diagram of enhanced AR signaling, bPSC proliferation and differentiation that are mediated through IL-1RA during prostate inflammation that mimics the non-bacterial prostatitis. (This image was made at Biorender.com)

Supplementary Files

This is a list of supplementary files associated with this preprint. Click to download.

- [bPSCARIL1RASupplementalmaterials11123.pdf](#)
- [bPSCARIL1RASupplementalTable311123.xlsx](#)